RSC Advances

PAPER

View Article Online
View Journal | View Issue

Check for updates

Cite this: *RSC Adv.*, 2018, **8**, 39854

A colorimetric and fluorescent chemosensor for Hg^{2+} based on a photochromic diarylethene with a quinoline unit

Shuli Guo, Congbin Fan, Gang Liu* and Shouzhi Pu*

Received 9th October 2018
Accepted 20th November 2018

DOI: 10.1039/c8ra08358d

rsc.li/rsc-advances

A new colorimetric and fluorescent 'on–off' chemosensor, **1O**, based on a photochromic diarylethene with a quinoline unit was designed and synthesized. The chemosensor **1O** demonstrated selective and sensitive detection of Hg^{2+} ions in the presence of other competitive metal ions in acetonitrile. The stoichiometric ratio of the sensor **1O** for Hg^{2+} was determined to be 1 : 1, and the limit of detection of the probe **1O** was calculated to be 56.3 nM for Hg^{2+}. In addition, a molecular logic circuit with four inputs and one output was successfully constructed with UV/vis light and metal-responsive behavior. ESI-MS spectroscopy, Job's plot analysis, and ^1H NMR titration experiments confirm the binding behavior between **1O** and Hg^{2+}.

Open Access Article. Published on 28 November 2018. Downloaded on 4/2/2026 3:54:47 PM.
This article is licensed under a Creative Commons Attribution-NonCommercial 3.0 Unported Licence.

1. Introduction

Nearly all heavy metals are toxic to human health and dangerous for the environment. In particular, Hg^{2+} is one of the major and most deadly heavy metal ions,[1–3] and is widely distributed in the water, air, and soil of everyday living environments.[4,5] The accumulation of mercury even at low concentrations can cause many deleterious effects,[6,7] including DNA damage, movement disorders, mitosis impairment, and serious damage to the nervous and endocrine organ systems.[8–15] Many methods to measure Hg^{2+} have been reported, including atomic absorption spectrometry (AAS), electrochemical sensing, inductively coupled plasma optical emission spectrometry (ICP-OES), voltammetry, and more.[16–20] However, these traditional methods have some common disadvantages, such as expensive specialized equipment, complicated sample preparation, and long assay times.[21–23] Thus, it is important to develop a facile, rapid, sensitive, and easy to use method for sensing mercury ions even at low concentrations.

Optical methods, colorimetric or fluorometric, are preferred methods owing to their operational simplicity, real time monitoring, high selectivity and sensitivity, and low detection limits.[24–31] In addition, optical probes for the determination of transition metal cations are popular because they can facilitate analyte detection in solutions by the naked eye[32,33] as well as in living cells by microscopy.[34–36] Actually, a lot of fluorescent sensors have been designed for the detection of Hg^{2+}, such as rhodamine,[37] oligothiophene,[38] pyrazoline,[39] coumarin.[40] Unfortunately, most of these sensors for the detection of Hg^{2+} still have weak points, such as synthetic difficulty, complex molecular structure, poor selectivity and high detection limit. Therefore, it is necessary to design and develop efficient and convenient Hg^{2+} sensors for their promising application potential in the environment.

Diarylethene derivatives, one of the most promising photo-switchable dyes have attracted considerable research interest due to their excellent photo reactivity, thermal stability, and fatigue resistance.[41–44] They can be used to construct photoswitches, logic circuits, optical memories, and chemosensors.[45–49] So far many diarylethene derivatives have been reported as optical sensors, such as diarylethene attach to 1-butyl-2-oxo-1,2-dihydroquinoline,[50] thieno-imidazole,[51] chromone,[52] 2-hydrazinopyridine,[53] 1,8-naphthyridin,[54] rhodamine 6G.[55] However, most of these diarylethene derivatives are designed for detection of Zn^{2+}, Al^{3+}, Cd^{2+} with Schiff base structure, and the reported sensing methods combining the colorimetric and fluorometric are relatively sparsely, especially with a quinoline group. Meanwhile, to our knowledge, Schiff base is unstable.[56] Thus, it is still highly desirable to design sensitive and stable sensors for Hg^{2+} detection, which taking both advantages of colorimetric and fluorometric methods based on diarylethene with quinoline group.

Toward this goal, we describe herein a colorimetric and fluorescent chemosensor for Hg^{2+} based on photochromic diarylethene with a quinoline unit. The selectivity and sensitivity for Hg^{2+} were systematically investigated, and the results indicated that **1O** exhibited changes in both absorbance and fluorescence upon exposure to Hg^{2+} ions over other competing metal ions. In addition, **1O** could detect Hg^{2+} ions with a low detection limit (56.3 nM). Scheme 1 shows the synthetic route and photochromic process of **1O**.

Jiangxi Key Laboratory of Organic Chemistry, Jiangxi Science and Technology Normal University, Nanchang 330013, PR China. E-mail: pushouzhi@tsinghua.org.cn; Fax: +86 791 83805212; Tel: +86 791 83805212; +86 791 83831996

This journal is © The Royal Society of Chemistry 2018

Open Access Article. Published on 28 November 2018. Downloaded on 4/2/2026 3:54:47 PM.
This article is licensed under a Creative Commons Attribution-NonCommercial 3.0 Unported Licence.

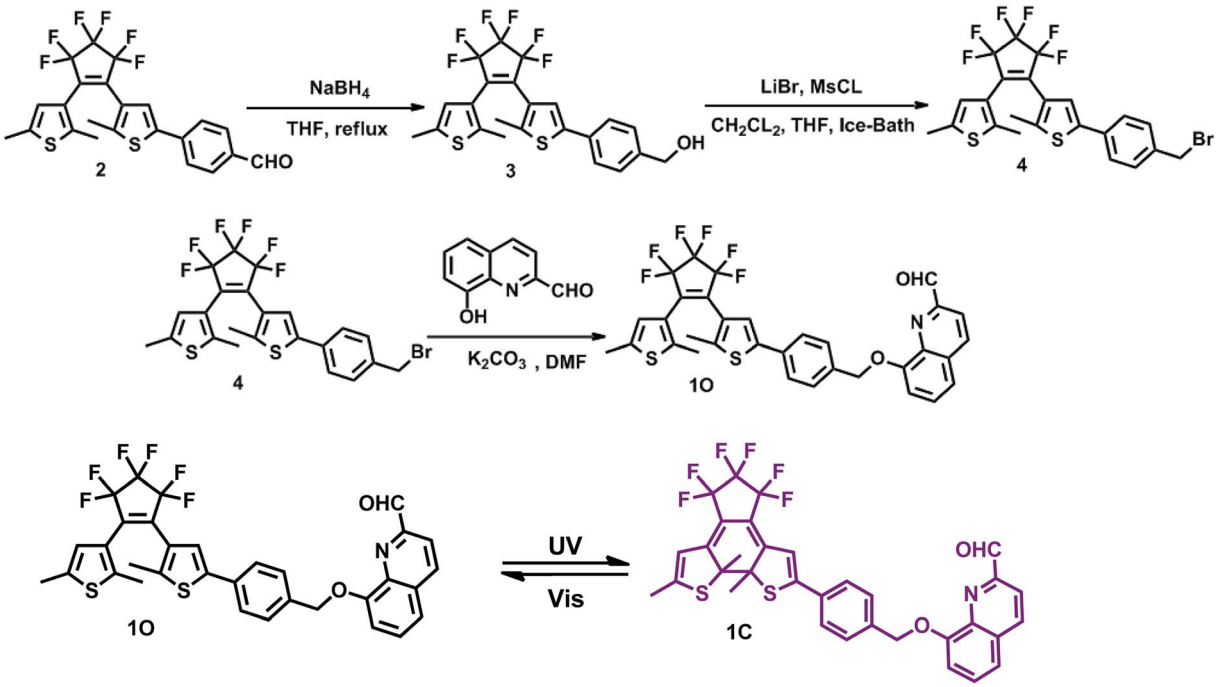

Scheme 1 Scheme of the synthesis of diarylethene **1O** and its photochromism.

2. Experiments

2.1. General methods

All solvents were of analytical grade and distilled before use. 8-Hydroxyquinoline was obtained from J & K Scientific Ltd and other chemical reagents were used as received. All metal ions expect for Ba^{2+} and K^{+} that were prepared with their chloride salts. Hg^{2+} was prepared with its high chloride salts, and the remainings were obtained by dissolving the corresponding metal nitrates (0.1 mmol) in distilled water (10 mL). An EDTA solution was prepared with ethylenediaminetetraacetic acid disodium salt (Na_2EDTA) (1.0 mmol) in distilled water (10 mL).

^{1}H NMR and ^{13}C NMR spectra were recorded on a Bruker AV400 spectrometer (400 MHz) using CD_3CL and CD_3CN as solvents and tetramethylsilane (TMS) as the internal standard. Mass spectra were obtained using an Agilent 1100 Ion Trap LC/MS MSD system. Melting points were measured using a WRS-1B melting point apparatus. Infrared spectra (IR) were collected on a BrukerVertex-70 spectrometer. UV-vis absorption spectra were recorded on an Agilent 8453 UV/vis spectrophotometer equipped with an MUA-165 UV lamp and MVL-210 visible lamp for photoirradiation. Fluorescence spectra were measured with a Hitachi F-4600 fluorescence spectrophotometer. Fluorescence quantum yield was measured using a QY C11347-11 absolute PL quantum yield spectrometer. Photoirradiation was performed on a setup consisting of a SHG-200 UV lamp, Cx-21 ultraviolet fluorescence analysis cabinet, and BMH-250 visible lamp. The synthetic route to the target compound **1O** is shown in Scheme 1. Intermediate compounds **2** were prepared by the reported method.[57]

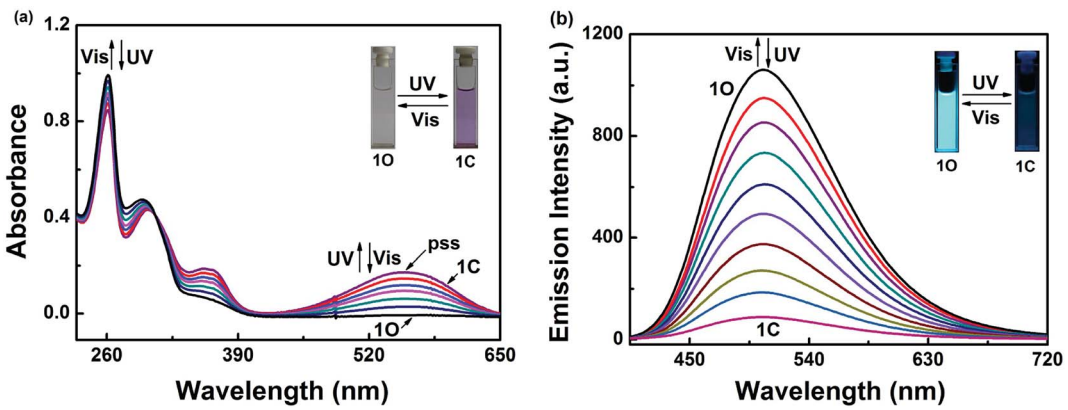

Fig. 1 Upon irradiation with UV-vis light: (a) absorption spectra changes of **1O** in acetonitrile (2.0×10^{-5} mol L^{-1}); (b) fluorescence spectra changes of **1O** in acetonitrile (2.0×10^{-5} mol L^{-1}). Excitation: 370 nm.

Open Access Article. Published on 28 November 2018. Downloaded on 4/2/2026 3:54:47 PM.
This article is licensed under a Creative Commons Attribution-NonCommercial 3.0 Unported Licence.

2.1.1 Synthesis of 1-(2,5-dimethyl-3-thienyl)-2-[2-methyl-5-(4-hydroxymethylphenyl)-3-thienyl]perfluorocyclopentene (3). 1.95 g, 4 mmol of compound **2** and 0.19 g, 4.8 mmol of $NaBH_4$ were taken in 50 mL of THF in a 100 mL round bottom flask. The mixture was stirred and refluxed for 2 h. After the reaction completed, the reaction product was cooled to RT and quenched with 20 mL water. The product was extracted with dichloromethane, the organic phase was washed with water, dried over anhydrous Na_2SO_4, filtered, and rotary evaporated. Finally, the compound was purified by column chromatography (petroleum ether : ethyl acetate = 1 : 1) to obtain a white solid 1.84 g (3.76 mmol, 94%). Mp: 353–354 K; ^{1}H NMR (DMSO, 400 MHz), δ (ppm): 1.843 (s, 3H, $-CH_3$), 1.902 (s, 3H, $-CH_3$), 2.293 (s, 3H, $-CH_3$), 4.495 (t, 2H, $-CH_2-$), 5.25 (s, 1H, –OH), 6.818 (s, 1H, Ar–H), 7.35 (d, 2H, Ar–H), 7.413 (s, 1H, Ar–H), 7.560 (d, 2H, Ar–H).

2.1.2 Synthesis of 1-(2,5-dimethyl-3-thienyl)-2-[2-methyl-5-(4-bromomethylphenyl)-3-thienyl]perfluorocyclopentene (4). To a stirred solution of 40 mL anhydrous CH_2Cl_2 in ice bath, compound **3** (1.47 g, 3.00 mmol), MsCl (0.39 mL, 4.80 mmol) and TEA (0.75 mL, 5.40 mmol) were added. After rapid stirring for ten minutes at 273 K, added 10 mL of anhydrous THF containing LiBr (1.03 g, 12.00 mmol) to the reaction flask. Keep

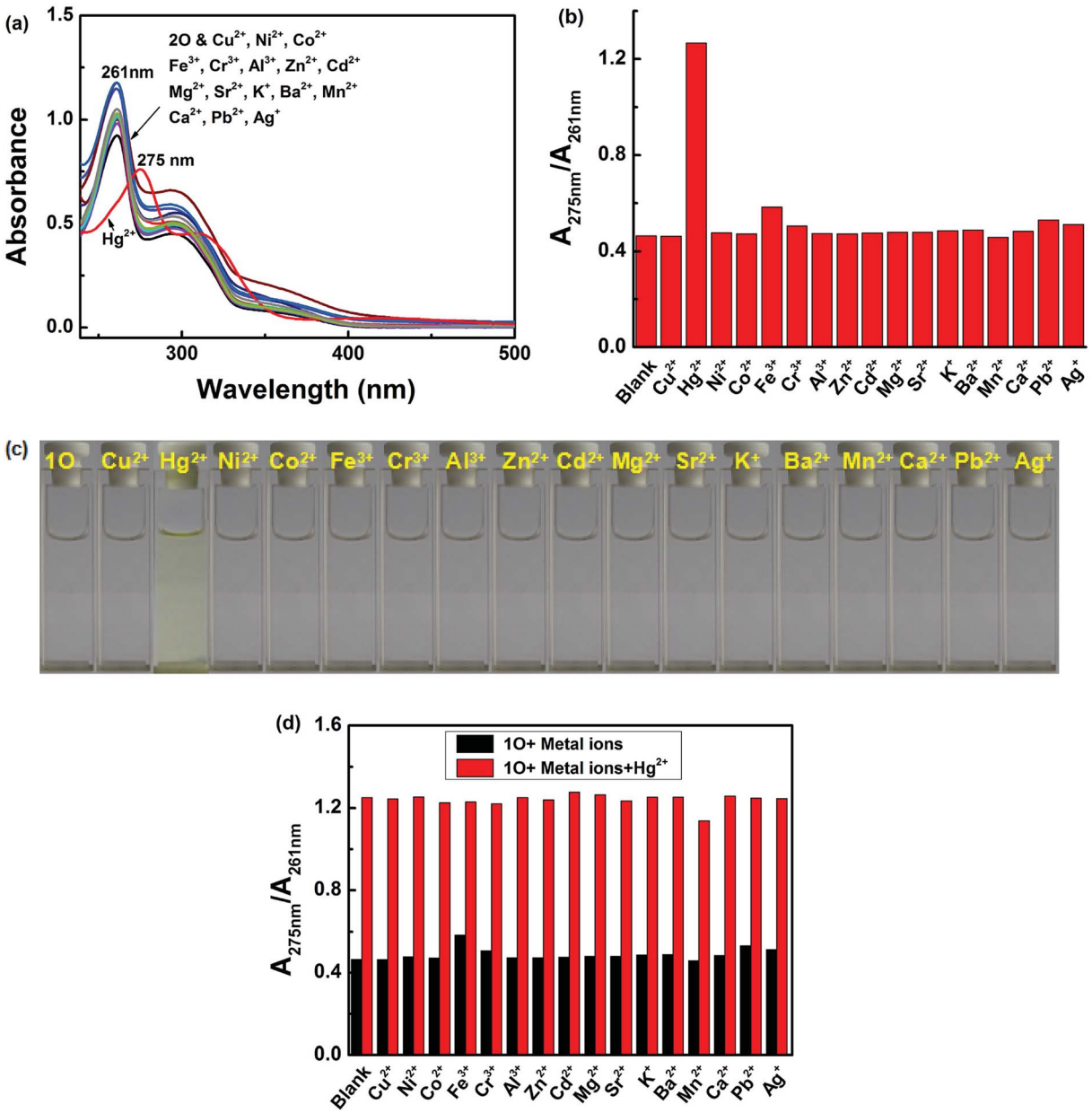

Fig. 2 Changes in the absorption of **1O** induced by various metal ions (1.0 equiv.) in acetonitrile (2.0×10^{-5} mol L^{-1}). (a) UV/vis absorption spectra of **1O** in the presence of different metal ions; (b) corresponding absorbance ratios ($A_{275\ nm}/A_{261\ nm}$) of **1O** in the presence of different metal ions; (c) photos demonstrating the color of **1O** solutions containing different metal ions; (d) competitive tests for the absorption response of **1O** in the presence of Hg^{2+} and other competing metal ions in acetonitrile. Black bars represent the absorption of **1O** solution in the presence of 1.1 equiv. metal ions and red bars represent the absorptions of **1O** solutions containing the metal ions and Hg^{2+} (1.0 equiv.).

This journal is © The Royal Society of Chemistry 2018

Open Access Article. Published on 28 November 2018. Downloaded on 4/2/2026 3:54:47 PM.
This article is licensed under a Creative Commons Attribution-NonCommercial 3.0 Unported Licence.

this temperature and continue to stir for 30 minutes. Then, the solution was warmed to room temperature and stirred for 12 h. After reaction, the product was quenched with 20 mL water and evaporated of organic solvents. Extracted with dichloromethane, dried over anhydrous Na_2SO_4, filtered, and rotary evaporated. Finally, the product was purified by column chromatography (petroleum ether : ethyl acetate = 8 : 1) to obtain a white solid 1.48 g (2.68 mmol, 90%). Mp: 345–346 K; ^{1}H NMR (DMSO, 400 MHz), δ (ppm): 1.556 (s, 3H, –CH_3), 1.927 (s, 3H, –CH_3), 2.412 (s, 3H, –CH_3), 4.763 (d, 2H, –CH_2–), 6.837 (s, 1H, Ar–H), 7.497 (d, 3H, Ar–H), 7.631 (t, 2H, Ar–H).

2.1.3 Synthesis of 1-(2,5-dimethyl-3-thienyl)-2-{2-methyl-5-phenyl-4-(2-formylquinoline-8-methoxyl)-3-thienyl} perfluorocyclopentene (1O). Compound **4** (0.55 g, 1 mmol) and 8-hydroxyquinoline-2-carboxaldehyde (0.19 g, 1.10 mmol) were added to anhydrous CH_3CN (30 mL) containing K_2CO_3 (0.33 g, 2 mmol). The solution was stirred at 283 K for 48 h. The reaction mixture was filtered, and the solvent was removed under vacuum. The crude product was purified by column chromatography on silica gel using dichloromethane/ethyl acetate (v/v = 6/1) as the eluent to give the target compound **1O** as a purple solid (0.42 g, 0.67 mmol) in 67% yield. Mp: 339–341 K. ^{1}H NMR (400 MHz, $CDCl_3$), δ (ppm): 1.88 (s, 3H, –CH_3), 1.94 (s, 3H, –CH_3), 2.45 (s, 3H, –CH_3), 5.53 (s, 2H, –CH_2–), 6.76 (s, 1H, Ar–H), 7.18 (d, 1H, Ar–H), 7.53 (t, 2H, Ar–H), 5.9 (t, 5H, Ar–H), 8.12 (d, 1H, Ar–H), 8.32 (d, 1H, Ar–H), 10.36 (s, 1H, –CHO); ^{13}C NMR (400 MHz, $CDCl_3$) δ (ppm): 14.34 (–CH_3), 15.07 (–CH_3), 29.69 (–CH_3), 70.81 (–CH_2–), 111.20, 117.92, 120.15, 122.76, 124.68, 125.86, 127.75, 129.56, 131.43, 133.21, 135.31, 136.26, 137.28, 137.78, 139.78, 140.38, 141.26, 141.54, 151.70, 155.13, 193.82; IR (KBr, ν, cm^{-1}): 1272 (–C–O), 1704 (–CHO). Anal. calcd for $C_{33}H_{23}F_6NO_2S_2$: C, 61.58; H, 3.60; F, 17.71; N, 2.18; O, 4.97; S, 9.96; found: C, 61.53; H, 3.65; F, 17.74; N, 2.23; O, 4.91; S, 9.93. MS (m/z): Calculated for $C_{33}H_{23}F_6NO_2S_2$ $[M]^+$: 643.11, found: 666.0972 for $[\mathbf{1O} + Na]^+$ and 698.1233 for $[\mathbf{1O} + 3H_2O + H]^+$.

3. Results and discussion

3.1. Photochromic and fluorescent properties of diarylethene 1O

The photochromic behavior of diarylethene **1O** induced by UV/vis light was monitored in acetonitrile ($C = 2.0 \times 10^{-5}$ mol L^{-1}) at room temperature. As shown in Fig. 1a, diarylethene **1O** displayed a sharp absorption band at 261 nm ($\varepsilon_{max} = 4.9 \times 10^4$ mol^{-1} L cm^{-1}), which is assigned to the π–π* transition. Upon irradiation with 297 nm light, the absorption band at 279 nm was decreased significantly. A new absorption band centered at 557 nm ($\varepsilon_{max} = 0.9 \times 10^4$ mol^{-1} L cm^{-1}) appeared and the color of the solution changed from colorless to purple due to the formation of ring-closed isomer **1C**.[58,59]

This photocyclization reaction reached the photostationary state (PSS) after 3 min of irradiation with UV light, where a clear

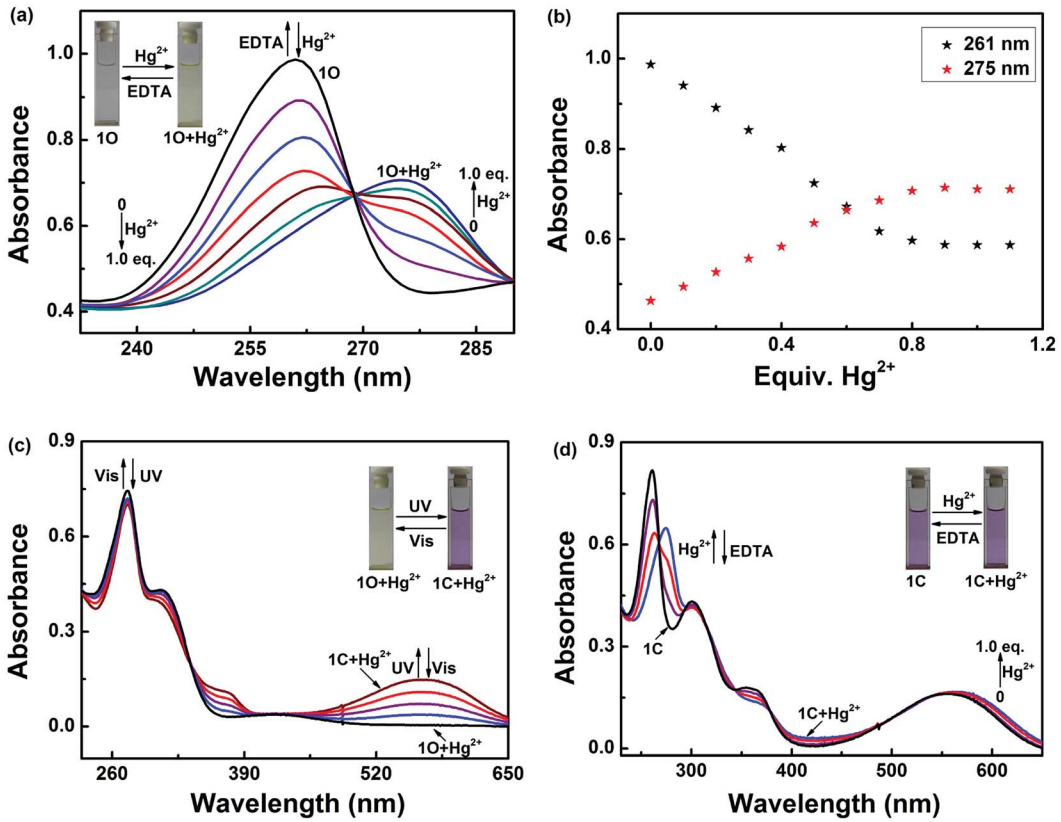

Fig. 3 Changes in the absorption spectrum and color of **1O** (2.0×10^{-5} moL L^{-1}) in acetonitrile induced by Hg^{2+}/EDTA and light stimuli: (a) UV/vis spectra of **1O** induced by Hg^{2+}/EDTA; (b) absorbance at 261 and 275 nm *versus* the concentration of Hg^{2+}; (c) UV/vis spectra of **1O** + Hg^{2+} induced by UV/vis light; (d) UV/vis spectra of **1C** induced by Hg^{2+}/EDTA.

Open Access Article. Published on 28 November 2018. Downloaded on 4/2/2026 3:54:47 PM.
This article is licensed under a Creative Commons Attribution-NonCommercial 3.0 Unported Licence.

isosbestic point was observed at 308 nm. These observations suggest that the process is a two-component photochromic reaction. In addition, the purple solution of **1C** could be completely bleached upon irradiation with visible light ($\lambda > 500$ nm) and the absorption spectrum returned back to the initial state **1O**. The cyclization and cycloreversion quantum yields were calculated to be 0.533 and 0.023, respectively, with 1,2-bis(2-methyl-5-phenyl-3-thienyl)-perfluorocyclopentene as the reference.

Fig. 1b shows the fluorescence emission spectra of **1O** in acetonitrile (2.0×10^{-5} mol L^{-1}) under photoirradiation at room temperature. A strong fluorescence peak of **1O** centered at 506 nm was observed under excitation at 370 nm. Upon irradiation with 297 nm UV light, the compound **1O** showed notable fluorescent switching properties, where the emission peak of **1O** decreased significantly and the solution color changed from bright cyan to dark. In the photostationary state, the fluorescence was 92% quenched due to the formation of the non-fluorescent ring closed isomer **1C**. The weak fluorescence may be due to incomplete cyclization. The fluorescence quantum yield of **1O** to **1C** was determined to be 0.245 to 0.021. Back irradiation with appropriate visible light ($\lambda > 500$ nm) regenerated the open-ring isomer **1O** and restored the initial fluorescence.

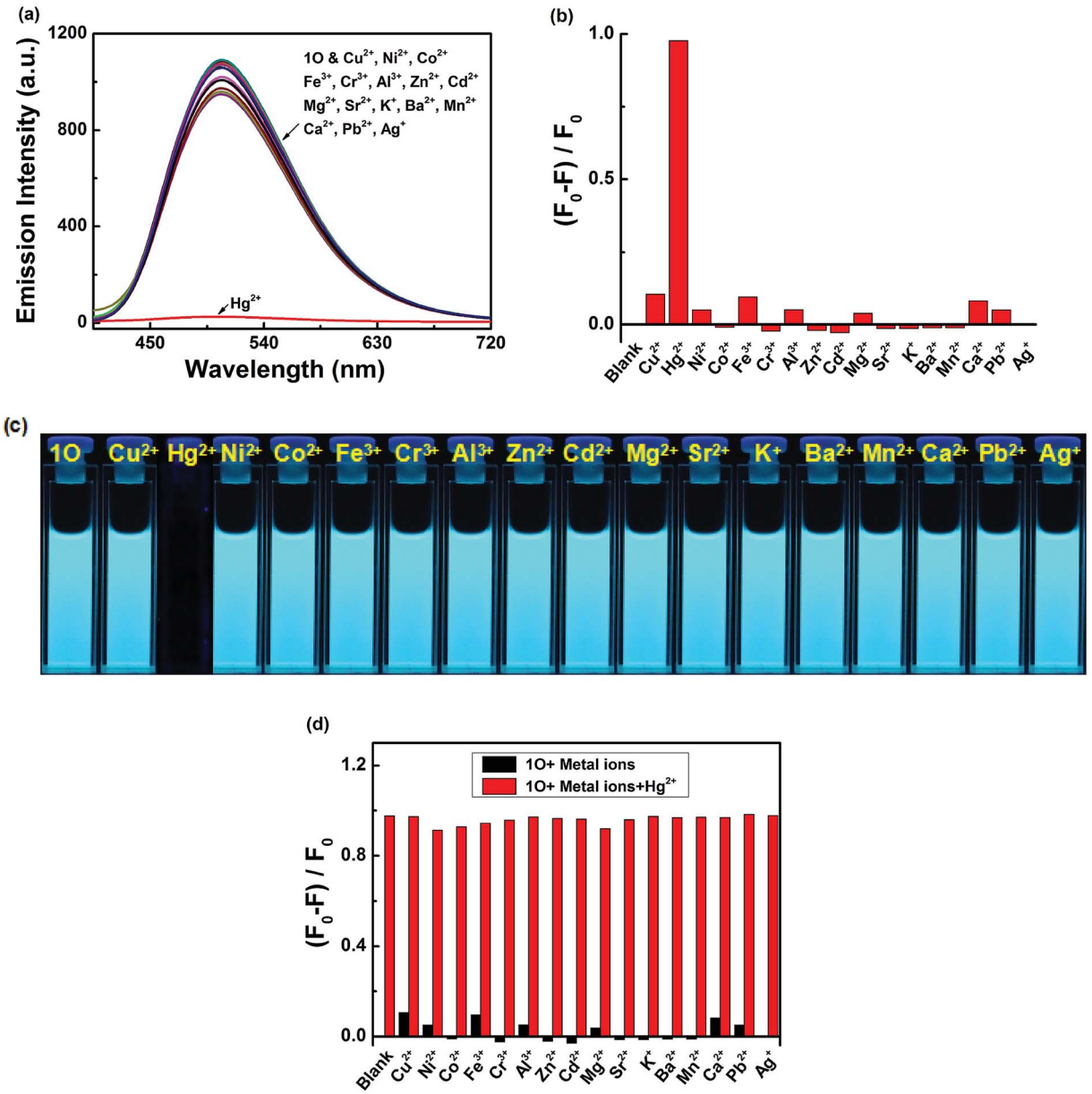

Fig. 4 Fluorescence responses of **1O** (2.0×10^{-5} mol L^{-1}) to various metal ions (2.1 equiv.) in acetonitrile. (a) Emission spectra of **1O** in the presence of different metal ions; (b) corresponding maximum emission intensities of **1O** in the presence of the metal ions; (c) photos demonstrating the colors of **1O** solutions containing different metal ions; (d) competitive tests for the fluorescent response of **1O** in the presence of Hg^{2+} and other competing metal ions in acetonitrile. Black bars represent the fluorescence of **1O** solution in the presence of 2.1 equiv. metal ions and red bars represent the fluorescence of **1O** solutions containing the metal ions and Hg^{2+} (2.1 equiv.).

This journal is © The Royal Society of Chemistry 2018

Open Access Article. Published on 28 November 2018. Downloaded on 4/2/2026 3:54:47 PM.
This article is licensed under a Creative Commons Attribution-NonCommercial 3.0 Unported Licence.

3.2. Absorption response of 1O to Hg^{2+}

Colorimetric sensing behavior of **1O** was examined by UV-vis in acetonitrile (2.0×10^{-5} mol L^{-1}) at room temperature. As shown in Fig. 2, compound **1O** was investigated in the presence of various metal ions, including Cu^{2+}, Hg^{2+}, Ni^{2+}, Co^{2+}, Fe^{3+}, Cr^{3+}, Al^{3+}, Zn^{2+}, Cd^{2+}, Mg^{2+}, Sr^{2+}, K^{+}, Ba^{2+}, Mn^{2+}, Ca^{2+}, Pb^{2+} and Ag^{+}. Of all of these ions, only Hg^{2+} caused a modest color change from colorless to yellow (Fig. 2c). The UV-vis spectra showed that Hg^{2+} addition to the sensor **1O** resulted in a 15 nm bathochromic shift from 261 nm to 275 nm, at the same time, a broad absorption band appeared in the visible region. These changes were ascribed to ligand-to-metal charge transfer (LMCT).[60–62] However, the other metal ions did not cause the absorption peak red shift and no new absorption band could be produced in the visible range (Fig. 2a). Fig. 2b shows the absorbance ratio ($A_{275\ nm}/A_{261\ nm}$) of **1O** upon addition of each ion, which also exhibited high selectivity of **1O** for Hg^{2+} ions. To explore the practical applications of **1O** in Hg^{2+} detection and to estimate the selectivity of **1O** for Hg^{2+}, competitive experiments were conducted with the metal ions listed above. As depicted in Fig. 2d, other competitive metal ions did not interfere with the recognition of Hg^{2+} ions, confirming the selectivity of the sensor **1O** for Hg^{2+} ions over other metal ions.

Fig. 3 shows the absorption spectral and color changes of **1O** in acetonitrile (2.0×10^{-5} moL L^{-1}) induced by the stimulation of Hg^{2+}/EDTA and UV/vis. As depicted in Fig. 3a, the first absorption band around 341 nm gradually reduced and a new absorption band at 275 nm obviously increased with the sequential addition of Hg^{2+} amount. It reached the maximum at 1.0 equiv. of Hg^{2+}, and a notable color change from colorless to yellow was apparent from bare eye. Further addition of Hg^{2+} did not change the absorption spectrum, suggesting that the **1O** + **Hg^{2+}** complex was formed. The absorbance intensity at 261 and at 275 nm exhibited a good linear relationship with the Hg^{2+} in the range of 0–1.0 equiv. (Fig. 3b).

Compound **1O** + **Hg^{2+}** could also undergo photoisomerization upon alternating irradiation with UV and visible light. Upon irradiation with 297 nm UV light, the yellow solution of **1O** + **Hg^{2+}** turned purple and a new absorption band centered at 532 nm ($\varepsilon_{max} = 7.4 \times 10^{3}$ moL^{-1} L cm^{-1}) emerged due to the formation of the closed-ring isomer **1C** + **Hg^{2+}** (Fig. 3c). In addition, **1C** + **Hg^{2+}** also could be formed by reacting **1C** with Hg^{2+} (Fig. 3d). It was noticed that the absorption properties of **1O** and **1C** could be restored by adding excess EDTA to the solutions containing **1O** + **Hg^{2+}** and **1C** + **Hg^{2+}**, respectively.

3.3. Fluorescence response of 1O to Hg^{2+}

As shown in Fig. 4, after the addition of 2.1 equiv. of different metal ions Cu^{2+}, Hg^{2+}, Ni^{2+}, Co^{2+}, Fe^{3+}, Cr^{3+}, Al^{3+}, Zn^{2+}, Cd^{2+}, Mg^{2+}, Sr^{2+}, K^{+}, Ba^{2+}, Mn^{2+}, Ca^{2+}, Pb^{2+} and Ag^{+}, no significant changes in fluorescence intensity were observed except for in case of Hg^{2+}, where an emission band peak at 506 nm exhibited quenching (Fig. 4a). Compared with that of **1O**, the fluorescence intensity of the complex **1O** + **Hg^{2+}** was reduced to 97% at 506 nm (Fig. 4b). Simultaneously, Hg^{2+} could make the color of the **1O** solution "switched-off" from a fluorescent bright cyan to a non-fluorescent color, no obvious color changes could be observed in the presence of other metal ions(Fig. 4c). These results suggest that **1O** is highly selective towards Hg^{2+}. To explore practical applicability of **1O** in Hg^{2+} detection, competitive experiments were performed in the presence of the above-mentioned metal ions (Fig. 4d). It was observed that the fluorescence quenching of **1O** + **Hg^{2+}** was not affected by the presence of other metal ions (2.1 equiv.) in acetonitrile, indicating the high binding affinity of **1O** for Hg^{2+}.

Meanwhile, changes in fluorescence of **1O** induced by Hg^{2+}/EDTA were performed in acetonitrile (2.0×10^{-5} mol L^{-1}) at room temperature, and the results are shown in Fig. 5. A decline in emission intensity at 506 nm was noted for **1O** when the Hg^{2+} concentration increased from 0 to 2.1 equiv., accompanied by a notable fluorescent color change from bright cyan to dark and followed by a plateau upon further titration. Notably, the fluorescence of **1O** was successfully restored with the addition of 2.1 equiv. of EDTA. In addition, the fluorescence quantum yield of **1O** + **Hg^{2+}** was determined to be 0.008, 29.6 folds lower than that

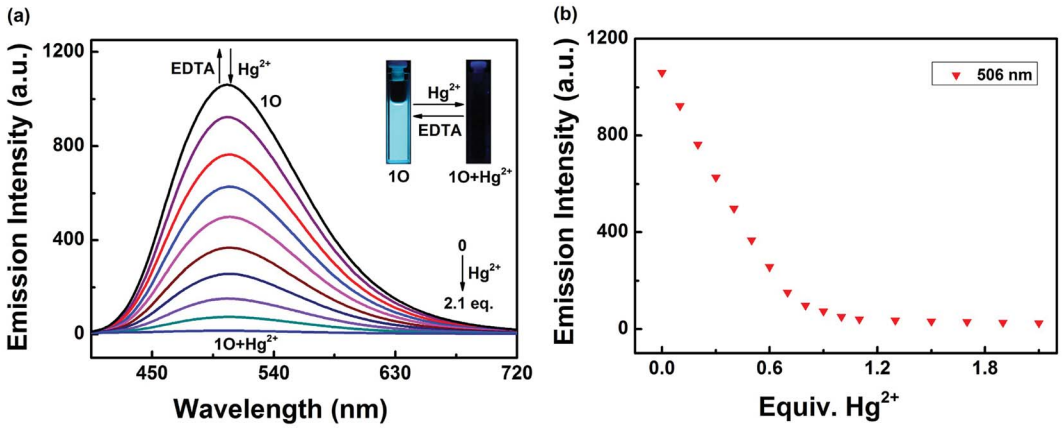

Fig. 5 Changes in the fluorescence of **1O** in acetonitrile (2.0×10^{-5} mol L^{-1}) induced by Hg^{2+}/EDTA, excited at 370 nm: (a) fluorescence emission spectra of **1O** titrated with different amounts of Hg^{2+}; (b) the fluorescence intensities of **1O** at 506 nm in the presence of different equiv. Hg^{2+}.

Open Access Article. Published on 28 November 2018. Downloaded on 4/2/2026 3:54:47 PM.
This article is licensed under a Creative Commons Attribution-NonCommercial 3.0 Unported Licence.

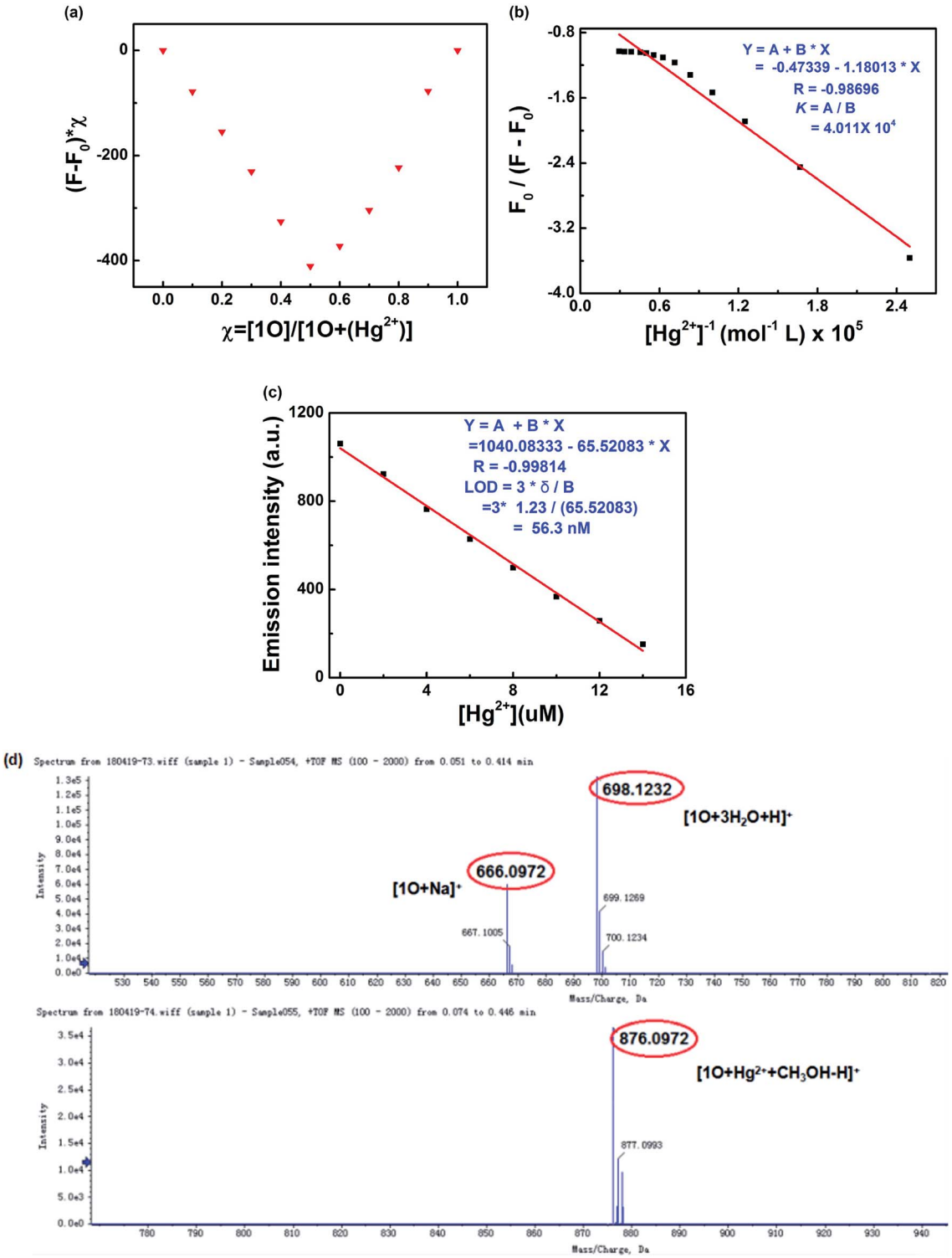

Fig. 6 (a) Job's plot showing the 1 : 1 complex of **1O** with Hg^{2+}; (b) Hildebrand–Benesi plot based on the 1 : 1 binding stoichiometry. The binding constant of **1O** with Hg^{2+} was calculated to be 4.011×10^4 L mol^{-1}; (c) the limit of detection (LOD was estimated to be 18.5 nM); (d) ESI-MS spectrum of **1O** and **1O** + Hg^{2+}.

of **1O** (Φ_f, **1O** = 0.245), suggesting that the diarylethene **1O** could also be potentially used as a fluorescent probe of Hg^{2+}.

The binding stoichiometry of **1O** and Hg^{2+} was calculated from the modified Hildebrand–Benesi equation. As shown in Fig. 6a, the lowest concentration of **1O** + Hg^{2+} was achieved at $[Hg^{2+}]/([Hg^{2+}] + [\mathbf{1O}]) = 0.5$, indicating that **1O** was bound to Hg^{2+} in a binding stoichiometry of 1 : 1. The association constant (K_a) of **1O** with Hg^{2+} was calculated to be 4.011×10^4 L

This journal is © The Royal Society of Chemistry 2018

Open Access Article. Published on 28 November 2018. Downloaded on 4/2/2026 3:54:47 PM.
This article is licensed under a Creative Commons Attribution-NonCommercial 3.0 Unported Licence.

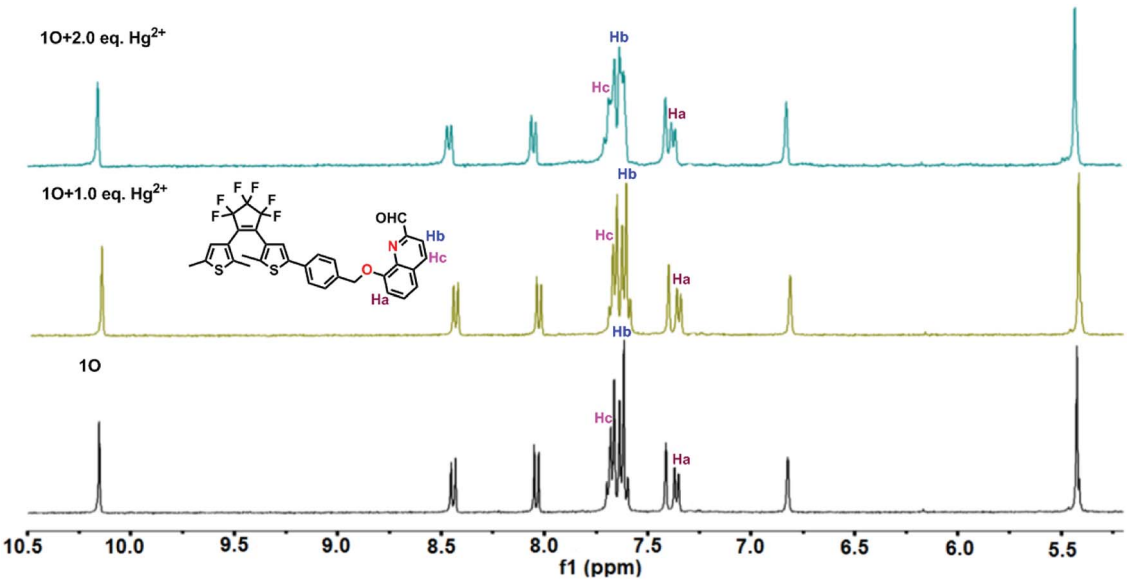

Fig. 7 ^{1}H NMR spectral changes in deuterated acetonitrile with the increasingly addition of Hg^{2+}.

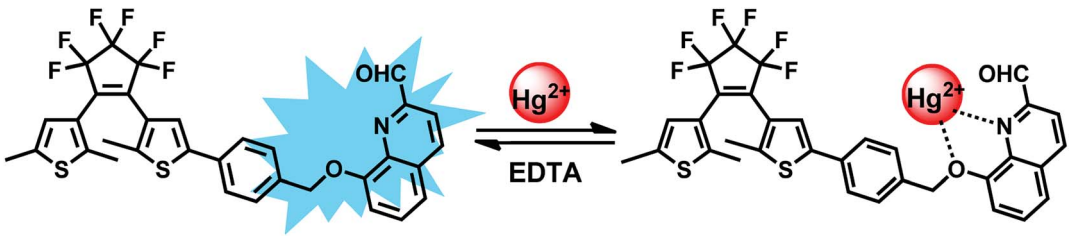

Scheme 2 The binding mode between **1O** and Hg^{2+}.

mol^{-1} ($R = -0.98696$) (Fig. 6b). The limit of detection of **1O** for Hg^{2+} was measured to be 56.3 nM (Fig. 6c), lower than those of other Hg^{2+} sensors reported in literature, suggesting that **1O** could be used as a highly sensitive fluorescence sensor of Hg^{2+}. The 1 : 1 coordination stoichiometry of **1O** with Hg^{2+} was further confirmed by the ESI mass spectrometry (ESI-MS) analysis. **1O** exhibited a characteristic peak at 666.0972 *m*/*z* for [**1O** + Na]$^+$ (calcd 666.11) and 698.1233 *m*/*z* for [**1O** + 3H_2O + H]$^+$ (calcd 698.11), which disappeared as 2.1 equiv. of Hg^{2+} were added, accompanied by the appearance of a new peak at 876.0972 *m*/*z* for [**1O** + **Hg^{2+}** + CH_3OH–H]$^+$ (calcd 876.10) (Fig. 6d).

Furthermore, ^{1}H NMR titrations verified the binding mode of **1O** with Hg^{2+}. As shown in Fig. 7, the double peaks at 7.353, 7.371 ppm belonging to Ha gradually shifted to 7.367 and 7.385 ppm, respectively. In addition, the proton signal of Hb at 7.617 ppm and Hc at 7.680 ppm reduced with the addition of Hg^{2+}. Therefore, we deduced that one oxygen atom close to methylene, and the nitrogen atom of quinolone together participated in binding with a Hg^{2+} ion, supporting that **1O** was an "O–N" type ligand. Similar phenomena also observed in other reported probes.[63] Based on the UV-vis and fluorescence titration experiments, Job's plot, ESI-MS, ^{1}H NMR titrations analysis, the proposed structure of **1O** + **Hg^{2+}** is shown in Scheme 2.

3.4. pH effects

In order to study practical applicability, the pH effect on the fluorescence intensity changes of the **1O** solution in the absence and presence of 2.1 equiv. of Hg^{2+} was evaluated. As shown in Fig. 8, when the pH value was lower than 4, it showed the fluorescence emission was significantly reduced, owing to the protonation of quinoline unit.[64] When the pH value range from 4 to 10, no apparent changes of the fluorescence intensity were

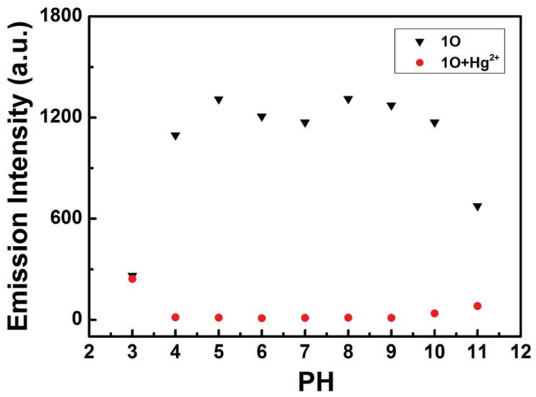

Fig. 8 Changes in the fluorescence intensity of sensor **1O** at 506 nm with and without Hg^{2+} at different pH values (λ_{ex} = 370 nm).

Open Access Article. Published on 28 November 2018. Downloaded on 4/2/2026 3:54:47 PM.
This article is licensed under a Creative Commons Attribution-NonCommercial 3.0 Unported Licence.

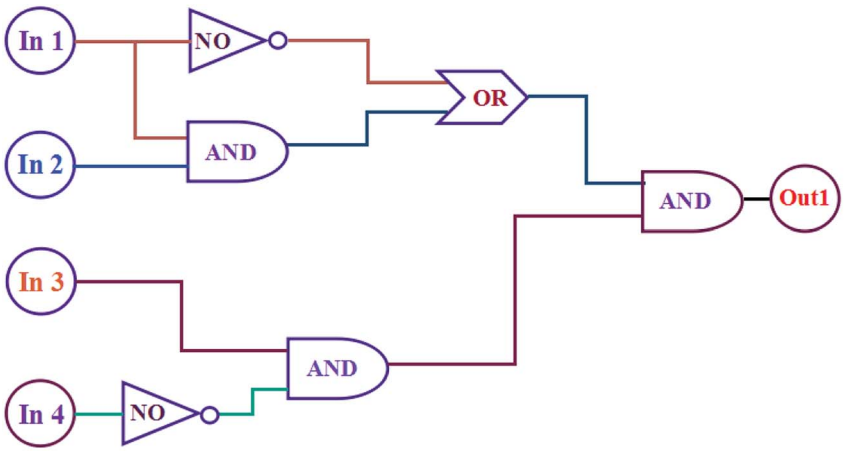

Fig. 9 The combinatorial logic circuits to the truth table given in Table 1: In1 (297 nm light), In2 (λ > 500 nm visible light), In3 (Hg^{2+}), In4 (EDTA) and output1 (fluorescence at 506 nm).

observed for **1O**. Coincidentally, the **1O** + Hg^{2+} complex was also not sensitive to pH in the range of 4–10, and at the same time, we can see the big gaps between the fluorescence intensity of **1O** and **1O** + Hg^{2+} within this pH range. Therefore, suggesting that sensor **1O** was stable at biological conditions and could detect Hg^{2+} in a relatively wide pH range (4 to 10).

3.5. Application in logic circuits

As mentioned above, the fluorescence of **1O** can be independently modulated by exposure to UV/vis light and to Hg^{2+}/EDTA. Based on these properties, a combinatorial logic circuit can be constructed using the stimulation of light irradiation (In1: 297 nm light and In2: λ > 500 nm visible light) and chemical compounds (In3: Hg^{2+} and In4: EDTA) as four input signals, and the fluorescence intensity at 506 nm as the output signal (Fig. 9). The output signal could serve as 'on' with a Boolean value of '1' when fluorescence intensity was quenched to *ca.* 97%, otherwise defined as 'off' with a Boolean value of '0'. For example, inputs of '0, 0, 1 and 0', corresponding to In1, In2, In3 and In4, result in an output of 'off, off, on and off'. Under these conditions, **1O** was converted to **1O** + Hg^{2+} by stimulation with Hg^{2+}, and its emission intensity was quenched dramatically. As a result, the output signal is 'on' and the output digit is '1'. All possible logical combinations of the four inputs and their corresponding outputs are listed in Table 1.

Table 1 Truth table for all possible strings of four binary-input data and the corresponding output[a]

Input				Output
In1 (UV)	In2 (Vis)	In3 (Hg^{2+})	In4 (EDTA)	λ_{em} = 506 nm
0	0	0	0	0
1	0	0	0	0
0	1	0	0	0
0	0	1	0	1
0	0	0	1	0
1	1	0	0	0
1	0	1	0	0
1	0	0	1	0
0	1	1	0	1
0	1	0	1	0
0	0	1	1	0
1	1	1	0	1
1	1	0	1	0
1	0	1	1	0
0	1	1	1	0
1	1	1	1	0

[a] At 506 nm, when fluorescence is quenched to *ca.* 97%, is defined as 1. Otherwise, it is 0.

4. Conclusion

In conclusion, we have developed a novel diarylethene-based colorimetric and on–off type fluorescent chemosensor **1O** for the selective and sensitive sensing of Hg^{2+} in acetonitrile. The complexation of **1O** with various metal ions was studied using UV-vis absorption and fluorescent emission spectra. Importantly, competition experiments suggested that the selective colorimetric and fluorescence quenching of Hg^{2+} is not affected by other metal ions. The detection limit of **1O** towards Hg^{2+} was 56.3 nM. These results showed that probe **1O** is an efficient sensor for detecting Hg^{2+}. In addition, the absorption and fluorescence emission of **1O** were efficiently adjusted by stimuli with light and chemical species. Based on these characteristics, an integrated logic circuit with multiple control switches was successfully designed and constructed.

Conflicts of interest

There are no conflicts of interest to declare.

Acknowledgements

The authors are grateful for the financial support from the National Natural Science Foundation of China (41867052, 21861017, 21662015, 41867053), the "5511" science and technology innovation talent project of Jiangxi, the key project of Natural Science Foundation of Jiangxi Province

 This journal is © The Royal Society of Chemistry 2018

(20171ACB20025), the Science Funds of Natural Science Foundation of Jiangxi Province (20171BAB203014, 20171BAB203011).

Open Access Article. Published on 28 November 2018. Downloaded on 4/2/2026 3:54:47 PM.
This article is licensed under a Creative Commons Attribution-NonCommercial 3.0 Unported Licence.

References

1 E. M. Nolan and S. J. Lippard, *Chem. Rev.*, 2008, **108**, 3443–3480.
2 T. Balaji, S. A. El-Safty, H. Matsunaga, T. Hanaoka and F. Mizukami, *Angew. Chem., Int. Ed.*, 2006, **118**, 7360–7366.
3 G. Sener, L. Uzun and A. Denizli, *Anal. Chem.*, 2014, **86**, 514–520.
4 C. J. Wu, J. B. Wang, J. J. Shen, C. Bi and H. W. Zhou, *Sens. Actuators, B*, 2017, **243**, 678–683.
5 Y. Zhang, J. J. Jiang, M. Li, P. F. Gao, L. H. Shi, G. M. Zhang, C. Dong and S. M. Shuang, *Sens. Actuators, B*, 2017, **238**, 683–692.
6 G. Q. Chen, Z. Guo, G. M. Zeng and L. Tang, *Analyst*, 2015, **140**, 5400–5443.
7 E. M. Nolan and S. J. Lippard, *Chem. Rev.*, 2008, **108**, 3443–3480.
8 Y. Wang, F. Yang and X. R. Yang, *Biosens. Bioelectron.*, 2010, **25**, 1994–1998.
9 Y. L. Wang, Y. Y. Cui, R. Liu, F. P. Gao, L. Gao and X. Y. Gao, *Sci. China: Chem.*, 2015, **58**, 819–824.
10 J. B. S. Fretham, S. Caito, J. E. Martinez-Finley and M. Aschner, *Toxicol. Res.*, 2012, **1**, 132–138.
11 P. S. Zhang, J. Li, B. W. Li, J. S. Xu, F. Zeng, J. Lv and S. Z. Wu, *Chem. Commun.*, 2015, **51**, 4414–4416.
12 J. S. Lee, M. S. Han and C. A. Mirkin, *Angew. Chem., Int. Ed.*, 2007, **46**, 4096.
13 T. Sun, Q. F. Niu, Y. Li, T. D. Li and H. X. Liu, *Sens. Actuators, B*, 2017, **248**, 24–34.
14 H. J. Huang, Y. Xu and X. Qian, *J. Org. Chem.*, 2009, **74**, 2167–2170.
15 R. Singh and G. Das, *Sens. Actuators, B*, 2018, **258**, 478–483.
16 H. Erxleben and J. Ruzicka, *Anal. Chem.*, 2005, **77**, 5124–5128.
17 Z. Q. Zhu, Y. Y. Su, J. Li, D. Li, J. Zhang, S. P. Song, Y. Zhao, G. X. Li and C. H. Fan, *Anal. Chem.*, 2009, **81**, 7660–7666.
18 M. Ozdemir, *Sens. Actuators, B*, 2017, **249**, 217–228.
19 J. M. Gong, T. Zhou, D. D. Song, L. Z. Zhang and X. L. Hu, *Anal. Chem.*, 2010, **82**, 567–573.
20 M. P. N. Bui, J. Brockgreitens, S. Ahmed and a. Abbas, *Biosens. Bioelectron.*, 2016, **85**, 280–286.
21 S. C. Lopes Pinheiro, I. M. Raimundo Jr, M. C. Moreno-Bondi and G. Orellana, *Anal. Bioanal. Chem.*, 2010, **398**, 3127–3138.
22 M. Ozdemir, *J. Photochem. Photobiol., A*, 2016, **31**, 7–13.
23 M. G. K. Salmani, G. H. Rounaghi and M. Chamsaz, *Sens. Actuators, B*, 2018, **256**, 968–975.
24 G. Q. Chen, Z. Guo, G. M. Zeng and L. Tang, *Analyst*, 2015, **140**, 5400–5443.
25 M. H. Lee, J. S. Kim and J. L. Sessler, *Chem. Soc. Rev.*, 2015, **44**, 4185–4191.
26 D. T. Quang and J. S. Kim, *Chem. Rev.*, 2010, **110**, 6280–6301.
27 K. P. Carter, A. M. Young and A. E. Palmer, *Chem. Rev.*, 2014, **114**, 4564–4601.
28 S. Y. Qin, B. Chen, J. Huang and Y. F. Han, *New J. Chem.*, 2018, **42**, 12766–12772.
29 J. F. Zhang, Y. Zhou, J. Yoon and J. S. Kim, *Chem. Soc. Rev.*, 2011, **40**, 3416–3429.
30 K. Ponnuvel, V. Padmini and R. Sribalan, *Sens. Actuators, B*, 2016, **222**, 605–611.
31 K. Ponnuvel, M. Kumar and V. Padmini, *Sens. Actuators, B*, 2016, **227**, 242–247.
32 J. M. Jung, C. Kim and R. G. Harrison, *Sens. Actuators, B*, 2018, **255**, 2756–2763.
33 Y. Zhao, L. L. Cui and Z. B. Chen, *Sens. Actuators, B*, 2017, **241**, 262–267.
34 H. Wang, P. S. Zhang, J. Chen, Y. Li, M. L. Yu, Y. F. Long and P. G. Yi, *Sens. Actuators, B*, 2017, **242**, 818–824.
35 S. M. Xu, Y. Liu, H. Yang, K. Zhao, J. G. Li and A. P. Deng, *Anal. Chim. Acta*, 2017, **964**, 150–160.
36 L. Yang, Y. A. Su, Y. N. Geng, H. Q. Xiong, J. L. Han, Q. Fang and X. Z. Song, *Org. Biomol. Chem.*, 2018, **16**, 5036–5042.
37 K. S. Min, R. Manivannan and Y. A. Son, *Sens. Actuators, B*, 2018, **261**, 545–552.
38 T. Sun, Q. F. Niu, Y. Li, T. D. Li and H. X. Liu, *Sens. Actuators, B*, 2017, **248**, 24–34.
39 E. Bozkurt and H. I. Gul, *Sens. Actuators, B*, 2018, **255**(1), 814–825.
40 C. J. Wu, J. B. Wang, J. J. Shen, C. Bi and H. W. Zhou, *Sens. Actuators, B*, 2017, **243**, 678–683.
41 M. Irie, T. Fukaminato and K. Matsuda, *Chem. Rev.*, 2014, **114**, 12174–12277.
42 W. L. Li, X. Li, Y. S. Xie, Y. Wu, M. Q. Li and X. Y. Wu, *Sci. Rep.*, 2015, **5**, 9186.
43 G. T. Xu, B. Li, J. Y. Wang, D. B. Zhang and Z. N. Chen, *Chem.–Eur. J.*, 2015, **21**, 3318–3326.
44 B. Li, H. M. Wen, J. Y. Wang, L. X. Shi and Z. N. Chen, *Inorg. Chem.*, 2015, **54**, 11511–11519.
45 J. J. He, J. X. He, T. T. Wang and H. P. Zeng, *J. Mater. Chem. C*, 2014, **2**, 7531–7540.
46 Y. L. Fu, C. B. Fan, G. Liu and S. Z. Pu, *Sens. Actuators, B*, 2017, **239**, 295–303.
47 S. J. Xia, G. Liu and S. Z. Pu, *J. Mater. Chem. C*, 2015, **3**, 4023–4029.
48 Y. Yamazaki, A. Sekine and H. Uekusa, *Cryst. Growth Des.*, 2017, **17**, 19–27.
49 R. J. Mart and R. K. Allemann, *Chem. Commun.*, 2016, **52**, 12262–12277.
50 E. T. Feng, Y. Y. Tu, C. B. Fan, G. Liu and S. Z. Pu, *RSC Adv.*, 2017, **7**, 50188.
51 Y. M. Xue, R. J. Wang, C. H. Zheng, G. Liu and S. Z. Pu, *Tetrahedron Lett.*, 2016, **57**, 1877–1881.
52 E. T. Feng, C. B. Fan, N. S. Wang, G. Liu and S. Z. Pu, *Dyes Pigm.*, 2018, **151**, 22–27.
53 S. Y. Li, D. B. Zhang, J. Y. Wang, R. M. Lu and C. H. Zheng, *Sens. Actuators, B*, 2017, **245**, 263–272.
54 X. X. Zhang, R. J. Wang, C. B. Fan, G. Liu and S. Z. Pu, *Dyes Pigm.*, 2017, **139**, 208–217.
55 H. T. Xu, H. C. Ding, G. Li, C. B. Fan, G. Liu and S. Z. Pu, *RSC Adv.*, 2017, **7**, 29827.

Open Access Article. Published on 28 November 2018. Downloaded on 4/2/2026 3:54:47 PM.
This article is licensed under a Creative Commons Attribution-NonCommercial 3.0 Unported Licence.

56 Z. L. Shi, Y. Y. Tu, R. J. Wang, G. Liu and S. Z. Pu, *Dyes Pigm.*, 2018, **149**, 764–773.
57 R. J. Wang, S. Z. Pu, G. Liu and S. Q. Cui, *Beilstein J. Org. Chem.*, 2012, **8**, 1018–1026.
58 C. B. Fan, L. L. Gong, L. Huang, F. Luo, R. Krashina, X. F. Yi, *et al.*, *Angew. Chem., Int. Ed.*, 2017, **56**, 7900–7906.
59 S. L. Guo, G. Liu, C. B. Fan and S. Z. Pu, *Sens. Actuators, B*, 2018, **266**, 603–613.
60 Y. Y. Fu, H. X. Li and W. P. Hu, *Eur. J. Org. Chem.*, 2007, **2007**, 2459–2463.
61 K. L. Zhong, X. Zhou, R. B. Hou, P. Zhou, S. H. Hou, Y. J. Bian, G. Zhang, L. J. Tang and X. H. Shang, *RSC Adv.*, 2014, **4**, 16612–16617.
62 Q. Li, Y. Guo and S. J. Shao, *Sens. Actuators, B*, 2012, **171–172**, 872–877.
63 L. L. Chang, Q. Gao, S. Liu, C. C. Hu, W. J. Zhou and M. M. Zheng, *Dyes Pigm.*, 2018, **153**, 117–124.
64 M. Amelia, M. Baroncini and A. Credi, *Angew. Chem., Int. Ed.*, 2008, **47**, 6240–6243.

This journal is © The Royal Society of Chemistry 2018